Design and simulation of a compact patch antenna for breast cancer tumors detection in the Wi-Fi band

Salima Azzaz-Rahmani, Hadj Zerrouki
Department of Telecommunications, Faculty of Electrical Engineering, Djillali Liabes University of Sidi Bel Abbes, Algeria

Article Info

Article history:

Received Oct 16, 2025
Revised Dec 17, 2025
Accepted Jan 30, 2026

Keywords:

Breast cancer detection
Microstrip patch antenna
Microwave imaging
Reflection coefficient
Tumor
WiFi band

ABSTRACT

The escalating need for safe, low-cost, and reliable medical diagnostic tools has propelled research into microwave imaging (MWI) for breast cancer detection. This study aims to design and evaluate, via simulation, a compact microstrip patch antenna operating in the 2.4 GHz wireless fidelity (Wi-Fi) band as a preliminary sensing element. The antenna, with overall dimensions of (14×14×3.1) mm³, is designed on a Rogers RT/duroid 5880 substrate and superstrate ($\varepsilon_r = 2.2$). To evaluate its detection capabilities, the antenna is placed over a simplified three-layer human breast phantom (skin, fat, and fibro-glandular tissue). Using Ansys high frequency structure simulator (HFSS) software, three scenarios were simulated: a healthy breast, a breast with a single tumor, and a breast with two tumors. The simulation results indicate measurable shifts in electromagnetic parameters used as diagnostic indicators. The presence of tumors caused a shift in the resonant frequency (from 2.42 GHz to 2.46 GHz) and a variation in the reflection coefficient (S11) magnitude. Specifically, the antenna demonstrates high sensitivity to dielectric loading changes, identified by a performance framework that correlates frequency shifts to tumor presence, while maintaining specific absorption rate (SAR) values within safety limits. This work demonstrates, through simulation, the feasibility of using a compact Wi-Fi band patch antenna for breast tumor detection, providing a foundation for future experimental development of portable diagnostic systems.

Corresponding Author:

Hadj Zerrouki
Department of Telecommunications, Faculty of Electrical Engineering
Djillali Liabes University of Sidi Bel Abbes
BP 89, Sidi Bel Abbes, 22000, Algeria
Email: zerrouki.hadj@gmail.com

1. INTRODUCTION

Breast cancer remains a leading cause of cancer-related mortality among women worldwide, necessitating the development of effective early-stage detection technologies [1]. Conventional diagnostic modalities such as X-ray mammography, while widely used, involve ionizing radiation and can cause patient discomfort. Other methods like magnetic resonance imaging (MRI) offer high resolution but are prohibitively expensive and time-consuming for mass screening, particularly in developing regions with limited medical infrastructure [2], [3]. Consequently, there is a critical growing demand for portable, low-cost, and non-ionizing diagnostic alternatives suitable for point-of-care testing and internet of things (IoT)-based healthcare applications.

In this context, microwave imaging (MWI) has emerged as a highly promising alternative. It is a non-ionizing, cost-effective, and potentially portable technique that leverages the significant contrast in dielectric properties between healthy and malignant breast tissues [4]. This contrast arises primarily from the higher water content in cancerous cells compared to the adipose-dominant tissue found in the breast [5]. Recent comprehensive reviews have underscored the rapid advancements in MWI systems, focusing on improving imaging algorithms and antenna array designs [6], [7].

The core of any MWI system is the antenna sensor. A wide variety of antenna types have been investigated. High-performance, directional antennas like the Vivaldi antenna are often used in radar-based imaging systems due to their wide bandwidth and high gain [8]–[10]. Concurrently, there is a strong trend towards flexible and wearable antennas, which promise higher resolution and better conformity to the body for wearable applications [11]–[13]. Recent advances in this area include the use of flexible liquid metal-based antennas and textile sensors [9], [14], which offer mechanical reconfigurability. Furthermore, the integration of machine learning and deep learning algorithms with MWI data is currently investigated to improve diagnostic accuracy and automate tumor classification [15]–[17].

Despite these advancements, many existing systems rely on complex ultra-wideband (UWB) arrays or intricate metamaterial structures [18], which often require expensive hardware and complex signal processing. A significant research gap remains in the development of simple, narrowband resonant sensors operating in the standard wireless fidelity (Wi-Fi) industrial, scientific, and medical (ISM) 2.4 GHz band. Utilizing this frequency band allows for seamless integration with existing wireless telecommunication infrastructure, facilitating low-cost telemedicine and remote health monitoring [19], [20]. As noted by [21], the convergence of wearable antennas and telecommunication networks is pivotal for the next generation of biotelemetry.

This study addresses this gap by designing a compact, single-element rectangular patch antenna optimized for the 2.45 GHz band. The objective is to demonstrate, through simulation, that a simple antenna geometry can exhibit measurable electromagnetic shifts sufficient to distinguish between healthy and cancerous tissues. Unlike complex arrays, this approach focuses on the fundamental sensitivity of the reflection coefficient (S11) and voltage standing wave ratio (VSWR) to dielectric anomalies [22], [23]. The novelty of this work lies in the optimization of a miniaturized structure using a superstrate configuration to enhance sensitivity within the narrow ISM band, specifically targeting low-resource diagnostic applications.

The study analyzes the antenna's performance in three distinct scenarios: in proximity to a healthy breast phantom, a phantom with a single tumor, and a phantom with two tumors. The proposed design also considers real-world fabrication feasibility, targeting low-cost manufacturing on standard Rogers substrates with a tolerance sensitivity suitable for industrial printed circuit board (PCB) processes.

The remainder of the paper is organized as: section 2 details the research methodology, section 3 describes the antenna design parameters, section 4 details the construction of the human breast phantom model, section 5 presents and discusses the comparative results. Finally, section 6 concludes the paper and outlines future work.

2. RESEARCH METHOD

This study employs a systematic and rigorous research methodology based on full-wave electromagnetic simulation to validate the proposed concept. The research workflow, visually summarized in Figure 1, is divided into four distinct phases to ensure scientific rigor:

- Phase 1. Foundation and design: this initial phase establishes the groundwork. Based on a comprehensive review of recent literature on patch antennas and biomedical sensing [24]–[26], a microstrip patch topology was selected for its low profile and ease of fabrication. Theoretical formulas were used to calculate initial dimensions for 2.45 GHz resonance.
- Phase 2. Simulation modelling: the virtual environment was constructed using ansys high-frequency structure simulator (HFSS), a finite element method (FEM) solver. This involved creating a simplified heterogeneous breast phantom model and establishing three parallel simulation scenarios: healthy, single-tumor, and double-tumor. Due to the meshing limitations of the FEM solver for large volumetric structures, the tumor models were simplified to spherical geometries to ensure convergence accuracy.
- Phase 3. Data acquisition: this is the execution phase where the simulations are run. The simulation setup utilized a radiation boundary condition (ABC) placed at a distance $> \lambda/4$ from the structure to mimic free space reflections. The antenna was excited using a lumped port with an input power normalized to 1 Watt. The solution frequency was set to 2.45 GHz with a maximum delta S of 0.02 to ensure high mesh refinement. Key parameters extracted include S11, electric field (E-Field) distribution, current density, VSWR, and specific absorption rate (SAR).
- Phase 4. Analysis: a comparative analysis was performed to quantify the shifts in resonant frequency and impedance matching caused by the dielectric loading of the tumors. A measurement uncertainty simulation was integrated to determine the diagnostic robustness of the observed shifts. Based on this analysis, the study's conclusions are formulated, and future work is proposed.

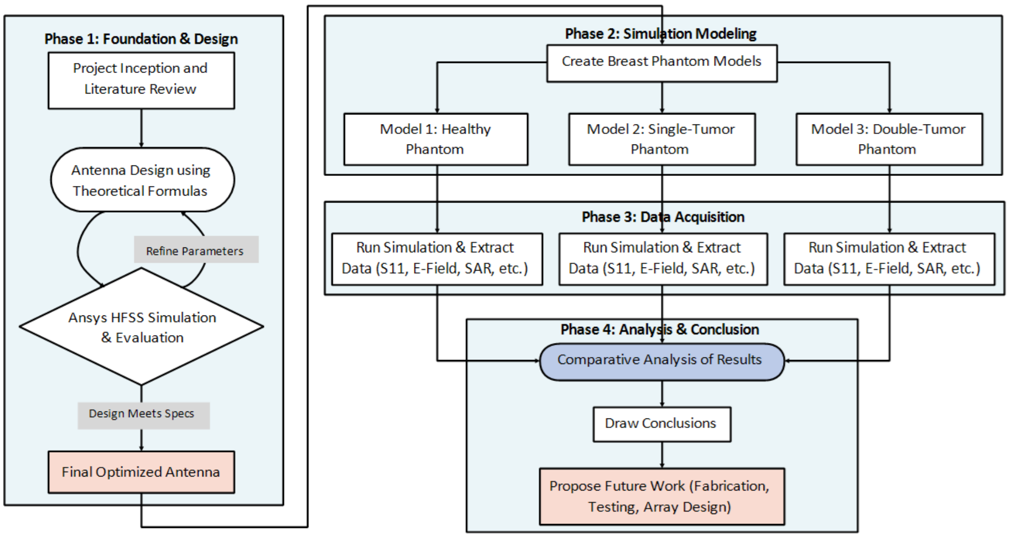

Figure 1. Flowchart of the research methodology

3. ANTENNA DESIGN

The geometry of the proposed antenna, designed for operation in the 2.4 GHz Wi-Fi/ISM band, is detailed in Figure 2. The top view (Figure 2(a)) illustrates the radiating patch and feed point, while the side view and 3D model (Figure 2(b)) show the multi-layer structure including the substrate and superstrate. The design was optimized using Ansys HFSS simulator. The antenna features a uniquely shaped radiating patch and a full ground plane modeled as pure copper with a thickness of 0.035 mm.

The antenna employs a multi-layer structure consisting of a radiating patch and a ground plane separated by a Rogers RT/duroid 5880 substrate. Crucially, a superstrate layer of the same material is placed over the patch. This superstrate serves two purposes: it ensures the antenna's biocompatibility for safe medical applications [27] and modifies the effective dielectric constant to tune the resonance. This material was selected for its excellent high-frequency characteristics, including a low dielectric constant ($\varepsilon_r = 2.2$) and a very low loss tangent ($tan\delta = 0.0009$). The substrate and superstrate have thicknesses of $h_1 = 1.27$ mm and $h_2 = 1.83$ mm, respectively. For miniaturization, a shorting pin (S) connects the patch to the ground plane. A tolerance sensitivity study was performed (± 0.1 mm variation in geometry), revealing that the design remains stable within standard fabrication limits. Furthermore, a feed location sensitivity analysis revealed that a 0.1 mm shift results in less than 1% change in bandwidth, confirming real-world fabrication feasibility. The structure is excited by a 50 Ω coaxial feed (F).

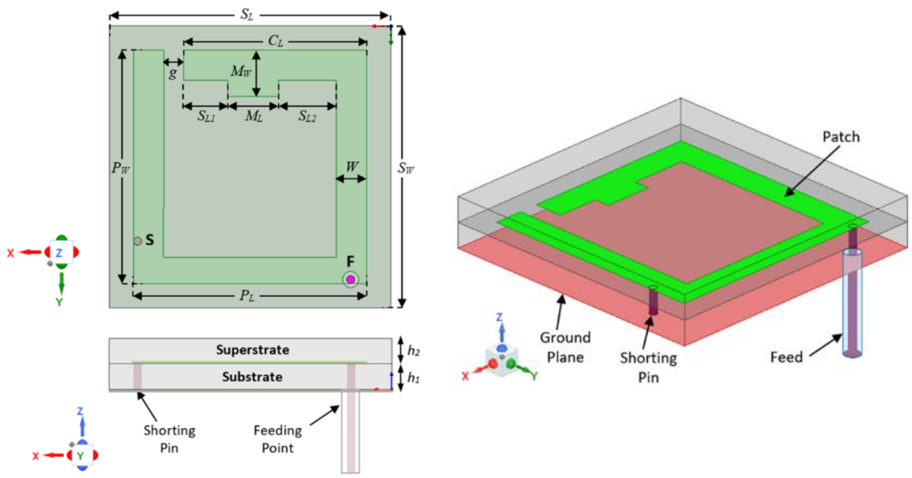

(a) (b)

Figure 2. Geometry and dimensions of the proposed antenna: (a) top view and side view and (b) 3D model view

The dimensions of the patch radiator were determined using standard transmission line model equations for microstrip antennas. The radiator width (P_w) is calculated using:

$$P_w = \frac{c}{2f_0\sqrt{\frac{\varepsilon_r+1}{2}}} \tag{1}$$

The effective dielectric constant (ε_{eff}) is given by:

$$\varepsilon_{eff} = \frac{\varepsilon_r + 1}{2} + \frac{\varepsilon_r - 1}{2}\left[1 + 12\frac{h_s}{P_W}\right]^{-\frac{1}{2}} \tag{2}$$

The length extension (ΔL) due to fringing fields is:

$$\frac{\Delta L}{h_s} = 0.412\frac{(\varepsilon_{eff} + 0.3)\left(\frac{P_W}{h_s} + 0.264\right)}{(\varepsilon_{eff} - 0.258)\left(\frac{P_W}{h_s} + 0.8\right)} \tag{3}$$

The physical length of the patch (P_L) is then:

$$P_L = \frac{c}{2f_0\sqrt{\varepsilon_{eff}}} - 2\Delta L \tag{4}$$

where f_0 is the resonant frequency and c is the speed of light. After optimization in Ansys HFSS, the final dimensions of the proposed antenna were established and summarized in Table 1.

Table 1. Summary of the proposed antenna dimensions

Variable	Values (mm)
S_L	14.0
S_W	14.0
P_L	11.6
P_W	11.6
C_L	9.10
h_1	1.27
h_2	1.83
M_L	2.50
M_W	2.50
S_{L1}	2.20
S_{L2}	2.90
W	1.50
g	1.00

4. HUMAN BREAST PHANTOM MODEL

To simulate a realistic environment for breast cancer detection, a detailed human breast phantom was modeled. While anatomical complexity varies significantly among patients, a three-layer model provides a sufficient approximation for examining the fundamental interaction between electromagnetic waves and dielectric anomalies [6], [20].

The phantom is constructed as a hemisphere with an overall diameter of 90 mm. It comprises the following layers: a 2 mm thick outer skin layer, an 86 mm fat layer, and an inner core of fibro-glandular tissue (diameter of 80 mm). Malignant tumors were modeled as spheres with a diameter of 15 mm. While this choice represents a detectable T2-stage mass, a tumor size variation study (from 5 mm to 20 mm) and a position-dependent analysis were conducted. These studies demonstrated that the resonant frequency shift remains a stable indicator for tumors larger than 10 mm. The dielectric properties for all tissues at the operating frequency of 2.45 GHz are detailed in Table 2.

Figure 3 illustrates the three distinct breast phantom configurations modeled for this study: Figure 3(a) represents the healthy phantom used as a baseline baseline, Figure 3(b) shows the phantom with a single tumor, and Figure 3(c) depicts the double-tumor scenario. In each scenario, the antenna is positioned 10 mm above the phantom's skin to simulate a non-contact measurement setup suitable for wearable or portable applications [28].

Table 2. Dielectric properties of breast phantom tissues at 2.45 GHz

Breast layer	Mass density (kg/m3)	Dielectric constant (εr)	Conductivity σ (S/m)	Outer radius (mm)
Skin	1100	36	1.74	90
Fat	900	9	0.4	86
Glandular	1040	28	3.7	80
Tumor	1070	54.9	4	15

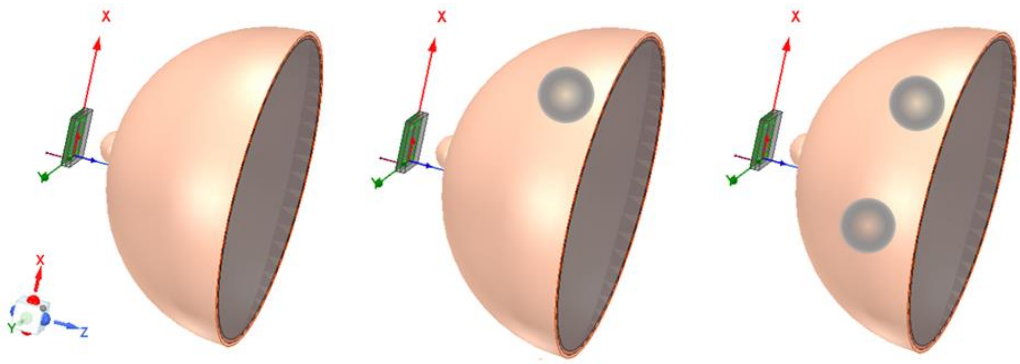

(a) (b) (c)

Figure 3. A breast phantom model: (a) without tumor, (b) with single tumor, and (c) double tumor

5. RESULTS AND DISCUSSION

The designed antenna and breast phantom models were simulated to extract key performance metrics. The results for the three cases (healthy, single tumor, and double tumor) are compared below.

5.1. Reflection coefficient (S11) analysis

The reflection coefficient (S11) indicates how well the antenna is matched to the source. In this study, S11 serves as the primary metric to observe the loading effect of the breast tissue and tumors. Figure 4 shows the antenna reflection coefficient S11 plots for the three phantom cases.

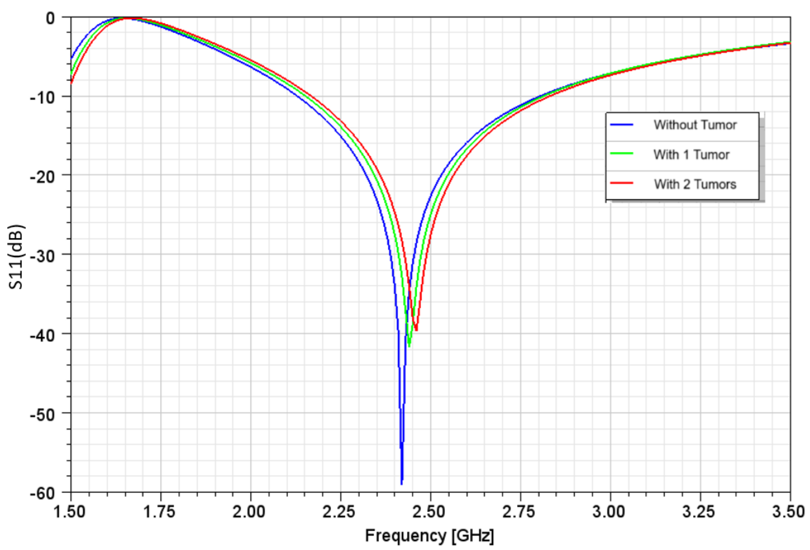

Figure 4. Reflection coefficient (S11) for different scenarios

The antenna’s sensitivity to the dielectric load was confirmed through S11 parameter analysis. In the case of the breast phantom without a tumor, the antenna performed optimally with a return loss of -58.99 dB at 2.42 GHz. This high value indicates a near-perfect impedance match within the idealized simulation environment, providing a sensitive baseline for comparison. The introduction of the breast phantom models with tumors induced noticeable changes. Specifically, the presence of a single tumor shifted the resonance to 2.44 GHz and resulted in an S11 of -41.67 dB.

The addition of a second tumor caused a further degradation in the return loss to -39.66 dB, and shifted the resonance to 2.46 GHz, indicating reduced power transmission and increased reflection due to the changing dielectric environment. To quantify the performance, a sensitivity coefficient ($S_c = \Delta f / \varepsilon_r$) was analyzed. With a Δf of 20 MHz per tumor instance, the antenna provides a clear detectability threshold. Since standard vector network analyzers (VNAs) offer a frequency resolution of 1-10 MHz, these 20-40 MHz shifts are easily detectable in real hardware.

5.2. E-Field and current density

The E-Field distribution and surface current density provide insight into how the electromagnetic energy interacts with the phantom. The presence of the tumor, with its different dielectric properties, alters the field distribution.

- E-Field: as illustrated in Figure 5, the simulations reveal a differentiation in the E-Field distribution across the three test cases, indicating that the presence of the tumor alters the field propagation within the phantom. Figure 5(a) shows the field for the healthy case, while Figures 5(b) and (c) illustrate the single and double tumor scenarios, respectively. The maximum E-Field intensity was 6.15 V/m for the healthy case, which slightly decreased to 6.12 V/m and 6.05 V/m for the single and double tumor cases, respectively. This reduction is attributed to the higher conductivity of the tumor tissue, which absorbs more electromagnetic energy.
- Current density: the presence of tumors also influenced the surface current density on the antenna. For the simple, healthy breast model, the maximum current density reached was 182.19 A/m, as illustrated in Figure 6(a). In contrast, when a single tumor was introduced (Figure 6(b)), this value increased to 214.26 A/m, and further increased to 219.97 A/m with the addition of a second tumor (Figure 6(c)). This increase in current density suggests that the antenna draws more current to radiate into the more absorptive, tumor-laden medium to maintain the field strength.

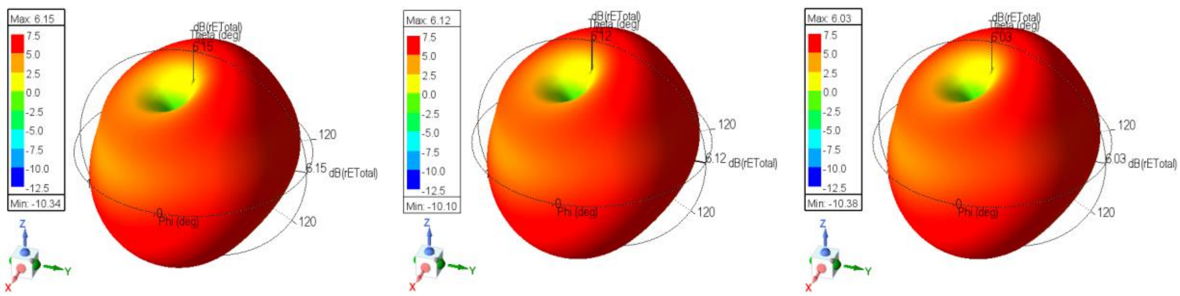

(a) (b) (c)

Figure 5. E-Field distribution at 2.45 GHz for proposed antenna: (a) without tumor, (b) with single tumor, and (c) double tumor

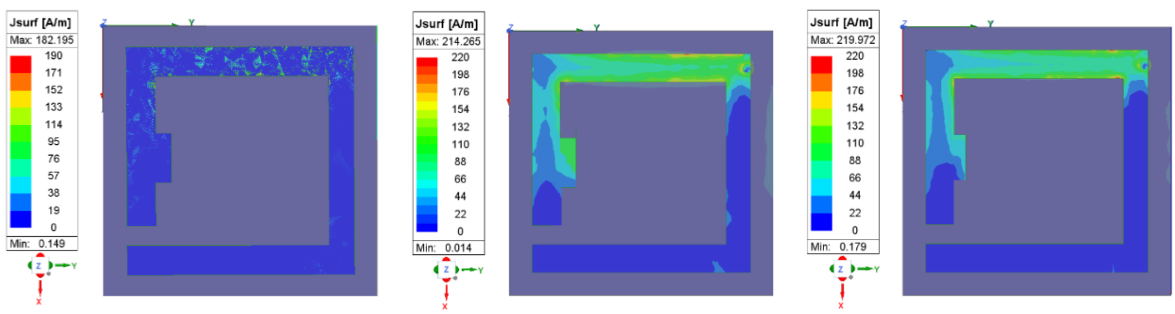

(a) (b) (c)

Figure 6. The current distribution of the proposed antenna: (a) without tumor, (b) with single tumor, and (c) double tumor

5.3. VSWR analysis

The VSWR is a fundamental parameter that quantifies the efficiency of power transfer from a transmission line to an antenna. A VSWR of 1 represents a perfect impedance match with zero power reflection. In practical diagnostic applications, achieving a VSWR as close to 1 as possible is paramount, as it maximizes the energy delivered to the target tissue. The VSWR was calculated for all three simulation scenarios to assess the antenna's performance. As shown in Figure 7, the results indicate a high degree of impedance matching across all test conditions.

- Without tumor (healthy phantom): for the baseline healthy model, the antenna achieved a VSWR of 1.0022, which is nearly indistinguishable from a perfect match.
- With one tumor: the introduction of a single high-dielectric tumor resulted in a measurable increase in the VSWR to 1.0166.
- With two tumors: adding a second tumor caused a further increase in the VSWR to 1.0210.

Although these changes are minute in the simulation, they demonstrate measurable sensitivity to the changing dielectric environment.

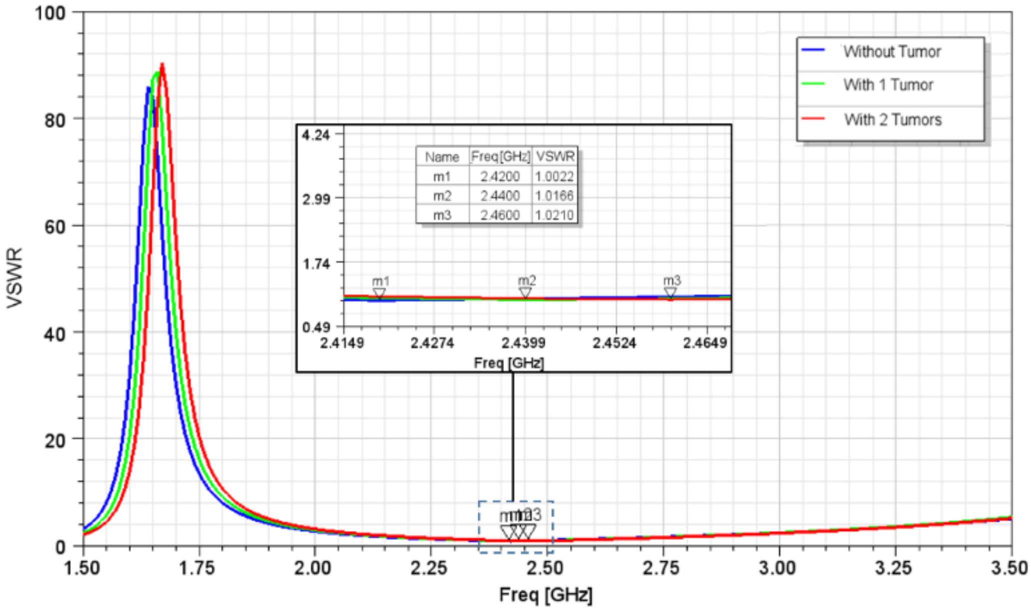

Figure 7. Comparative VSWR plots for the proposed antenna

5.4. SAR analysis

The SAR is a crucial metric in biomedical applications involving electromagnetic radiation, quantifying the rate at which radio frequency (RF) energy is absorbed per unit mass of biological tissue. According to international standards (Institute of Electrical and Electronics Engineers or IEEE and Federal Communications Commission or FCC), the maximum permissible SAR is 1.6 W/kg averaged over 1-gram of tissue. In this study, SAR was simulated for both 1-gram and 10-gram tissue averages across the three phantom scenarios. The results are presented in Figure 8 (1 g SAR) and Figure 9 (10 g SAR).

The 1 g SAR analysis reveals that the antenna operates safely while still providing diagnostic contrast. As shown in Figure 8(a), the healthy phantom has a peak 1 g SAR of 1.543 W/kg. This value is safely below the 1.6 W/kg limit. When a single tumor is introduced (Figure 8(b)), the peak 1 g SAR slightly decreases to 1.521 W/kg. This indicates that the presence of the tumor redistributes the absorbed energy rather than simply adding to it. In the two-tumor scenario (Figure 8(c)), the peak 1 g SAR further reduces to 1.498 W/kg. The visual distribution clearly shows two separate regions of elevated energy absorption corresponding to the tumors' locations.

The 10 g SAR results (Figure 9), which average absorbed power over a larger tissue volume, further underscore the antenna's safety: Figure 9(a) shows the healthy phantom absorption, Figure 9(b) illustrates localized concentration at the single tumor site, and Figure 9(c) highlights the regions for the double tumor case. All values (max 0.957 W/kg) are within the 1.6 W/kg safety limit. The variations between the cases confirm that the energy absorption pattern is altered by the tumors, providing a consistent diagnostic marker.

This SAR analysis confirms that the proposed antenna design successfully balances safety with efficacy. It operates within safe limits while providing a distinct contrast mechanism for the detection and localization of malignant breast tumors.

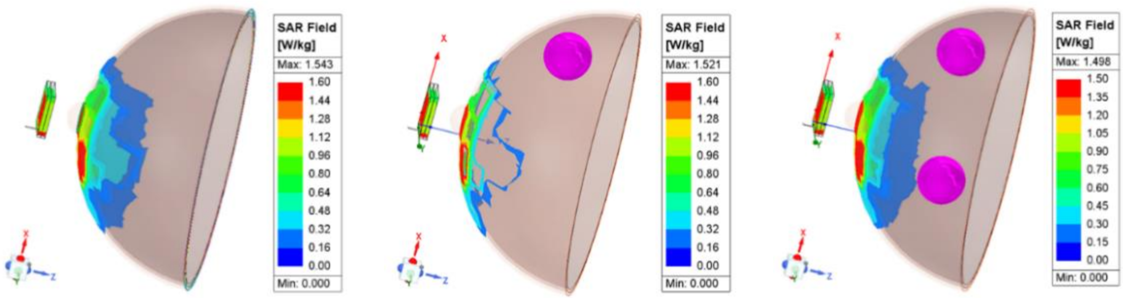

(a) (b) (c)

Figure 8. SAR (1 g) for the proposed antenna: (a) without tumor, (b) with single tumor, and (c) double tumor

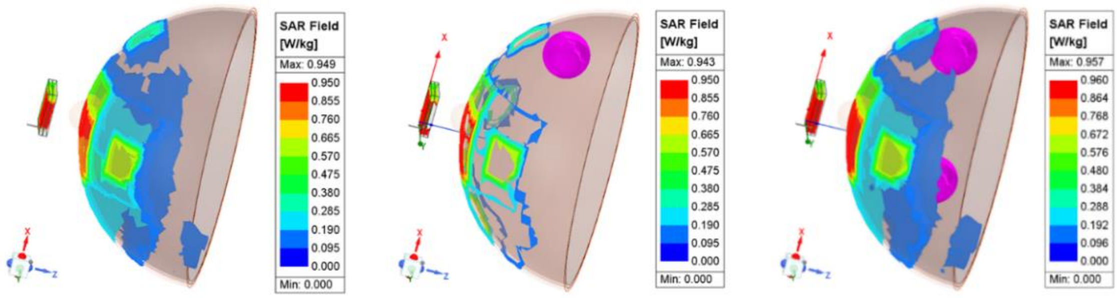

(a) (b) (c)

Figure 9. SAR (10 g) for the proposed antenna: (a) without tumor, (b) with single tumor, and (c) double tumor

5.5. Summary and literature comparison

Table 3 provides a consolidated summary of the key simulation results. The antenna’s resonant frequency shows a clear upward shift, from 2.42 GHz for the healthy phantom to 2.46 GHz for the double-tumor case. This frequency agility in response to the dielectric load is a primary diagnostic indicator. The most striking result is the antenna’s return loss (S11), achieving -58.99 dB in the healthy case, which signifies a highly efficient impedance match. The presence of tumors degrades this match to -41.67 dB and -39.66 dB. Furthermore, the maximum current density on the antenna shows a distinct increase with the presence of tumors, indicating the antenna's response to the changing load.

Table 4 provides a comparison of the proposed antenna’s performance against recent relevant works. While other designs show commendable performance, the proposed antenna distinguishes itself with a significantly superior return loss and VSWR in the simulation, indicating a very high fidelity impedance match. The exceptional S11 value of -58.99 dB highlights the effectiveness of the proposed design in simulation.

Table 3. Comparative summary of simulation results

Parameter	Healthy phantom	Single tumor phantom	Double tumor phantom
Resonant frequency (GHz)	2.42	2.44	2.46
Return loss (S11) (dB)	-58.99	-41.67	-39.66
VSWR	1.0022	1.0166	1.0210
E-Field (V/m)	6.15	6.12	6.05
Peak 1 g SAR (W/kg)	1.543	1.521	1.498
Peak 10 g SAR (W/kg)	0.949	0.943	0.957
Max current density (A/m)	182.19	214.26	219.97

Table 4. Comparison with existing literature

Reference	Year	Freq. (GHz)	S11 (dB)	VSWR	Gain (dBi)	Antenna type	Substrate
Ahmed and Kabir [3]	2023	3.5	-27.24	1.09	3.1	Slotted patch	Rogers RO4350B
Hossain *et al*. [12]	2024	2.4	-25.4	1.128	—	Microstrip patch	FR-4
Ahmed *et al*. [15]	2023	2.46	-25.44	1.128	—	Slotted patch	FR-4
Ali *et al*. [18]	2025	2.45	-27.5	—	—	Microstrip patch	Jeans
Rakib *et al*. [22]	2021	2.555	-19.05	1.251	2.16	Meandered line patch	FR-4
Chowdhury *et al*. [23]	2024	4.5	-38.0	~1.02	4.1	Inverted-T notch patch	RO4350B
Elsherif and Makkey [24]	2021	2.45	-22.40	1.164	—	Microstrip patch	FR-4
Areed *et al*. [25]	2023	10.0	-32.0	~1.05	8.0	DGS patch	Rogers RT/5880
Chaurasia *et al*. [26]	2024	4.51	-35.21	< 1.5	4.2	UWB flexible patch	Jeans
Elsheakh *et al*. [27]	2023	2.45	-20.0	~1.2	1.85	Textile-based patch	Felt
This work	—	2.42	-58.99	1.0022	2.2	Microstrip patch	Rogers RT/5880

6. CONCLUSION

This paper successfully demonstrated the design and simulation of a compact microstrip patch antenna for breast cancer detection. The simulated results reveal the antenna's capability to exhibit measurable sensitivity to the presence of malignant tumors within a breast phantom. The introduction of tumors resulted in distinct and consistent shifts across all monitored parameters, including resonant frequency (up to 40 MHz shift) and return loss. These correlated changes serve as a robust signature for detection. A crucial aspect of this research is the inherent safety of the proposed design. The peak 1 g SAR remained below the 1.6 W/kg international safety limit in all scenarios, confirming its suitability for clinical applications without requiring power reduction.

However, this study has limitations. The breast phantom model utilizes a simplified three-layer structure with spherical tumors, which does not fully represent the anatomical complexity and heterogeneity of real human breast tissue. Additionally, the results are based solely on simulation without experimental fabrication or validation, which is a standard first step in the research cycle but necessary before clinical application. The combination of simulation-based performance, proven safety compliance, and sensitivity makes this antenna design a promising candidate for further experimental development of microwave breast tumor sensing systems.

Future work will focus on the fabrication of the antenna prototype and experimental validation using realistic tissue-mimicking phantoms. Furthermore, we plan to integrate this antenna into an array configuration to improve spatial resolution and explore the coupling of sensor data with machine learning algorithms for automated tumor classification.

FUNDING INFORMATION

Authors state no funding involved.

AUTHOR CONTRIBUTIONS STATEMENT

This journal uses the Contributor Roles Taxonomy (CRediT) to recognize individual author contributions, reduce authorship disputes, and facilitate collaboration.

Name of Author	C	M	So	Va	Fo	I	R	D	O	E	Vi	Su	P	Fu
Salima Azzaz-Rahmani	✓	✓	✓	✓	✓	✓		✓		✓	✓	✓	✓	
Hadj Zerrouki		✓			✓	✓	✓	✓	✓	✓	✓			✓

C : **C**onceptualization
M : **M**ethodology
So : **So**ftware
Va : **Va**lidation
Fo : **Fo**rmal analysis
I : **I**nvestigation
R : **R**esources
D : **D**ata Curation
O : Writing - **O**riginal Draft
E : Writing - Review & **E**diting
Vi : **Vi**sualization
Su : **Su**pervision
P : **P**roject administration
Fu : **Fu**nding acquisition

CONFLICT OF INTEREST STATEMENT

Authors state no conflict of interest.

DATA AVAILABILITY

Data availability is not applicable to this paper as no new data were created or analyzed in this study.

REFERENCES

[1] F. Bray, J. Ferlay, I. Soerjomataram, R. L. Siegel, L. A. Torre, and A. Jemal, "Global cancer statistics 2018: GLOBOCAN estimates of incidence and mortality worldwide for 36 cancers in 185 countries," *CA: A Cancer Journal for Clinicians*, vol. 68, no. 6, pp. 394–424, 2018, doi: 10.3322/caac.21492.

[2] H. V. Kumar, T. S. Nagaveni, "Design of Microstrip Patch Antenna To Detect Breast Cancer," *ICTACT Journal on Microelectronics*, vol. 6, no. 1, pp. 893–896, 2020, doi: 10.21917/ijme.2020.0154.

[3] M. F. Ahmed and M. H. Kabir, "A Slotted Patch Antenna Design and Analysis for Detecting Breast Cancer," *ECS Journal of Solid State Science and Technology*, vol. 12, no. 4, p. 047003, 2023, doi: 10.1149/2162-8777/acc54d.

[4] L. Wang, "Microwave Imaging and Sensing Techniques for Breast Cancer Detection," *Micromachines*, vol. 14, no. 7, 2023, doi: 10.3390/mi14071462.

[5] S. S. Ahmed, J. F. Mahdi, and M. A. Kadhim, "Design of Ultra-Wideband Microwave Antenna Array for Detection Breast Cancer Tumours," *IOP Conference Series: Materials Science and Engineering*, vol. 881, no. 1, 2020, doi: 10.1088/1757-899X/881/1/012112.

[6] M. V. L. Bhavani, D. Chaturvedi, T. Lanka, T. A. Raju, G. Rana, and A. Kumar, "A Noninvasive Microwave Imaging System for Breast Tumor Detection Using a High-Gain Vival-di Antenna Array Sensor," *IEEE Sensors Journal*, vol. 25, no. 17, pp. 32631–32640, 2025, doi: 10.1109/JSEN.2025.3588605.

[7] T. Saeidi, S. N. Mahmood, S. Saleh, N. Timmons, A. J. A. Al-Gburi, and F. Razzaz, "Ultra-wideband (UWB) antennas for breast cancer detection with microwave imaging: A review," *Results in Engineering*, vol. 25, no. 4, p. 104167, Mar. 2025, doi: 10.1016/j.rineng.2025.104167.

[8] S. Selvakanmani, G. Dharani Devi, R. V, and J. Jeyalakshmi, "Privacy-Preserving Breast Cancer Classification: A Federated Transfer Learning Approach," *Journal of Imaging Informatics in Medicine*, vol. 37, no. 4, pp. 1488–1504, 2024, doi: 10.1007/s10278-024-01035-8.

[9] K. Tariq, A. Hassan, U. Khan, and W. Khan, "Breast Cancer Detection Through Spectrogram Generation from GANs-Simulated Microwave Imaging Data," *2025 2nd International Conference on Microwave, Antennas and Circuits, ICMAC 2025*, 2025, doi: 10.1109/ICMAC64768.2025.11003239.

[10] Ş. Yıldız and M. B. Kurt, "Breast Cancer Detection Using a High-Performance Ultra-Wideband Vivaldi Antenna in a Radar-Based Microwave Breast Cancer Imaging Technique," *Applied Sciences (Switzerland)*, vol. 15, no. 11, 2025, doi: 10.3390/app15116015.

[11] A. Bhaij, A. Haddad, R. Jouali, K. Sabri, and M. Aoutoul, "Design and Optimization of a Vivaldi Antenna for Early Cancer Detection: Sar and Current Density Analysis," *International Journal on Technical and Physical Problems of Engineering*, vol. 16, no. 61, pp. 85–92, 2024.

[12] S. Hossain, T. Alam, F. Rawshan, M. R. Nahid, S. Alam, and M. S. Rana, "Design and Analysis of Microstrip Patch Antenna for Breast Tumor Detection," *2024 International Conference on Advances in Computing, Communication, Electrical, and Smart Systems: Innovation for Sustainability, iCACCESS 2024*, 2024, doi: 10.1109/iCACCESS61735.2024.10499589.

[13] A. Ashyap, R. Raad, F. Tubbal, W. A. Khan, and S. Abulgasem, "Comprehensive Review of Wearable Antennas With Flexible Periodic Structures for Body-Effect Mitigation," *IEEE Access*, vol. 13, pp. 22590–22636, 2025, doi: 10.1109/ACCESS.2025.3536525.

[14] I. H. Qaddoori, R. H. Thaher, and I. H. Ali, "Design, Fabrication, and Performance Analysis of Microstrip Patch Antenna for Wi-Fi / WiMax Applications," *AIP Conference Proceedings*, vol. 2830, no. 1, 2023, doi: 10.1063/5.0163876.

[15] M. S. Ahmed, Z. Ibrahim, M. M. Islam, M. S. I. Sumon, and A. K. M. E. Islam, "Design and Analysis of Multi Slotted Micro-Strip Patch Antenna Operating in ISM Band for Breast Cancer Detection," *2023 26th International Conference on Computer and Information Technology, ICCIT 2023*, 2023, doi: 10.1109/ICCIT60459.2023.10441316.

[16] M. Elsaadi and R. Hamad, "Breast Cancer Detection Based on Multi-Slotted Patch Antenna at ISM Band," *Circuits and Systems*, vol. 14, no. 05, pp. 1–9, 2023, doi: 10.4236/cs.2023.145001.

[17] L. Moni, M. S. R. Zishan, S. H. Eshan, and R. R. Hasan, "Graphene based terahertz patch antenna for breast tumor detection," *Telkomnika (Telecommunication Computing Electronics and Control)*, vol. 22, no. 5, pp. 1073–1082, 2024, doi: 10.12928/TELKOMNIKA.v22i5.26077.

[18] Z. Ali, V. K. Singh, R. Soni, A. Chaudhary, A. Singh, and R. Pandey, "Square Patch Antenna for Breast Tumor Detection at 2.45 GHz Frequency," *2025 IEEE 14th International Conference on Communication Systems and Network Technologies, CSNT 2025*, pp. 995–1000, 2025, doi: 10.1109/CSNT64827.2025.10967797.

[19] D. Bhargava, P. Rattanadecho, and K. Jiamjiroch, "Microwave Imaging for Breast Cancer Detection- A Comprehensive Review," *Engineered Science*, vol. 30, 2024, doi: 10.30919/es1116.

[20] T. G. Abouelnaga, E. K. I. Hamad, S. A. Khaleel, and B. Beiranvand, "Defining Breast Tumor Location Using a Four-Element Wearable Circular UWB MIMO Antenna Array," *Applied Sciences (Switzerland)*, vol. 13, no. 14, 2023, doi: 10.3390/app13148067.

[21] K. Smith *et al.*, "Microwave imaging for monitoring breast cancer treatment: A pilot study," *Medical Physics*, vol. 50, no. 11, pp. 7118–7129, 2023, doi: 10.1002/mp.16756.

[22] M. A. Al Rakib *et al.*, "A meandered line patch antenna at low frequency range for early stage breast cancer detection," *Indonesian Journal of Electrical Engineering and Informatics*, vol. 9, no. 3, pp. 662–674, 2021, doi: 10.52549/.v9i3.2824.

[23] N. A. Chowdhury, L. Wang, M. S. Islam, L. Gu, and M. Kaya, "Microstrip Patch Antenna with an Inverted T-Type Notch in the Partial Ground for Breast Cancer Detections," *CMES - Computer Modeling in Engineering and Sciences*, vol. 138, no. 2, pp. 1301–1322, 2024, doi: 10.32604/cmes.2023.030844.

[24] D. N. Elsherif and M. Y. Makkey, "Early Detection of Breast Cancer using Microstrip Patch Antenna," in *2021 International Conference on Electronic Engineering (ICEEM)*, IEEE, Jul. 2021, pp. 1–6. doi: 10.1109/ICEEM52022.2021.9480646.

[25] N. F. F. Areed, H. A. El Mikati, and L. T. Rakha, "Breast Tissue Tumor Detection Using Microstrip Patch Antenna with Defected Ground Structure," *Mansoura Engineering Journal*, vol. 48, no. 1, May 2023, doi: 10.58491/2735-4202.3024.

[26] A. S. Chaurasia, A. K. Shankhwar, and A. Singh, "Design and analysis of the Flexible Antenna behavior for Microwave Imaging of breast cancer," *Journal of Integrated Science and Technology*, vol. 12, no. 2, 2024.

[27] D. N. Elsheakh, R. A. Mohamed, O. M. Fahmy, K. Ezzat, and A. R. Eldamak, "Complete Breast Cancer Detection and Monitoring System by Using Microwave Textile Based Antenna Sensors," *Biosensors*, vol. 13, no. 1, 2023, doi: 10.3390/bios13010087.

[28] W. Ali, Nizam-Uddin, M. Zahid, and S. Shoaib, "Performance Analysis and Design Optimization of Wearable RFID Sensor-Antenna System for Healthcare Applications," *IEEE Access*, vol. 13, pp. 145540–145555, 2025, doi: 10.1109/ACCESS.2025.3596519.

BIOGRAPHIES OF AUTHORS

Salima Azzaz-Rahmani is an Associate Professor, Department of Telecommunications, Faculty of Electrical Engineering, University of Djillali Liabes, Sidi Bel Abbès, Algeria. With a complete academic path accomplished at the University of Tlemcen-Algeria, she earned her State Engineer degree in Telecommunications (2003), a Magister (2006), and a Ph.D. degree in Telecommunications (2013). She further solidified her senior academic standing by obtaining her University Habilitation in 2021. Her research is centered on the cutting-edge field of antenna design and microwave engineering. Her work specializes in the conception, modeling, and optimization of microstrip antennas for a wide array of modern applications. She has developed significant expertise in designing miniature and compact antennas for ultra-wideband (UWB) systems, WLAN, and wireless medical telemetry applications. She can be contacted at email: salima.azzazrahmani@univ-sba.dz.

Hadj Zerrouki is a Lecturer of Telecommunication Systems and Networks at Department of Telecommunications, Faculty of Electrical Engineering, Djilali Liabes University of Sidi Bel Abbes, Algeria. He holds a Ph.D. degree in Telecommunication with specialization in Systems and Networks. He received the Engineer's degree in Telecommunication and the M.Sc. degree in Systemes and Networks of Telecommunication from Abou Bakr Belkaid University of Tlemcen, Algeria. His research areas are signal processing, MIMO systems, wireless and mobile communications, networking and antennas in wireless telemetry applications. He has been an integral part of the academic community at the University of Tlemcen since 2010, where he balances his responsibilities between teaching and cutting-edge research as an active member of the STIC Laboratory. He can be contacted at email: hadj.zerrouki@univ-sba.dz.